

MACROMOLECULAR COMPOUNDS
AND POLYMERIC MATERIALS

Cross-Linking in the Molecular Structure of Poly(vinyl butyral) and Properties Investigation

Majid Abdouss^a, Aref Shokri^{b,*}, and Sayed Hossein Sayed Yaghoubi^a

^a Chemical Group, Amirkabir University of Technology, Tehran, 334-64615 Iran

^b Jundi-Shapur Research Institute, Dezful, 334-64615 Iran

*e-mail: aref.shokri3@gmail.com

Received November 12, 2021; revised December 27, 2021; accepted December 30, 2021

Abstract—The poly(vinyl butyral) (PVB) is a resin that is used in areas where strong adhesion, optical transparency, multi-surface adhesion, hardness and flexibility are required. The purpose of this research is to cross-link the bonds in this polymer by benzoyl peroxide as a type of peroxide. The oxygen-oxygen bond of benzoyl peroxide was fragmented to produce two radicals by heating, and a hydrogen atom was separated from the hydroxyl group, and subsequently, the reaction of oxygen radical to acetylated carbon in the vinyl butyral monomer and forming a cross-link had happened. The properties of the cross-linked polymer were investigated and compared with linear polymer. Chemical identification tests such as Fourier transform infrared spectroscopy (FT-IR), X-ray diffraction pattern (XRD), scanning electron microscope (SEM) and differential scanning calorimeter (DSC), also mechanical tests including, Shore D Hardness test, impact and tensile test were applied. Through characterization and physical tests, it can be concluded that the cross-linked polymer had more resistance and can distribute the impact force better, endured more stress and also exhibited greater toughness, denser in color, more adhesion, and higher crystallinity than the linear polymer.

Keywords: poly(vinyl butyral), Shore D Hardness test, cross-linked polymer, benzoyl peroxide

DOI: 10.1134/S1070427221120077

INTRODUCTION

Some polymers such as polyethylene (PE), polyvinyl chloride (PVC), polypropylene (PP) and so on were used in industry as an insulator, adhesives etc. They have low cost, a simple production process and a wide range of required properties at room temperature. The mentioned polymers can be simply molded in many shapes at greater temperatures, which are mainly plastic in nature [1]. Nowadays, the main challenge in polymer technology is the used methods for relating polymers properties to their structures [2]. In this article, the properties of plasticized poly(vinyl butyral) (PVB) that is frequently used in safety products and laminated glass were investigated [3]. In 1944, an American scientist, Robert Burke, first produced the polyvinyl alcohol with butanol in an aqueous medium in the presence of a strong acid catalyst during the condensation reaction and then prepared the precipitated poly(vinyl butyral) from the solution in the acetalization process [4]. Poly(vinyl butyral) is a copolymer that

belongs to the group of thermoplastics. The percentage of monomers in this polymer varies between 78–85% vinyl butyral monomer, 2–5% acetate monomer, and 10–20% vinyl alcohol monomer. Monomers are soluble in a variety of organic and inorganic solvents, and this property also results in high adhesion to different surfaces. Naturally, since the vinyl butyral monomer is more non-polar than the other two monomers, it can be more hydrophobic in high percentage and can resist water [5]. In addition, the PVB has exceptional moisture resistivity, good mechanical features, dielectric features, and good adhesion to particles [6–8]. Other properties of PVB include transparency against light, good flexibility while having high hardness and impact resistance, high pigmentation and production capability [9].

One of the usages of PVB is for coating which attracted more notice due to its exceptional film-forming, heat resistance, impact resistance and high tensile. Meanwhile, the active sites for chemical reactions were produced due to the existence of OH groups in PVB structures and

the potential for production of composite by chemical treatment was increased. In this field, Luckachan et al. were added chitosan on mild carbon steel and fabricated anti-corrosion coatings of PVB were produced [10].

Some researchers filled the composite materials based on PVB medium by silica, montmorillonite, barium titanate, and glass-ceramic powders in the manufacture of various functional materials [11]. Zhou et al. investigated that the nanocomposites of PVB/vermiculite and PVB were gained by in-situ reaction of polyvinyl alcohol [12].

The nanocomposites morphology and microwave absorption characteristics of polyvinyl butyral (PVB)-MnO₂ was inspected by Bora et al., and they realized that the nanocomposite of PVB-MnO₂ had a very high loss factor (got up to 84%) and therefore, for numerous microwave-based claims it can be considered as a new microwave absorbing covering substantially [13]. Also, Zaw Oo et al. explored the influence of polyvinyl acetals on the possessions of an epoxy oligomer and found that the impact features were improved by about 2 times through using modifiers, whereas the residual strength pointers change slightly [14].

In this study, the PVB was thermally cross-linked by Benzoyl peroxide through a radical mechanism. The characterizations and physical and mechanical tests were performed to compare the linear polymer with cross-linked ones and finally, the advantages of cross-linked polymer were presented according to the experimental results.

EXPERIMENTAL

Materials. In this work, poly(vinyl butyral) (PVB) with an average molecular weight of 53 000 g/mol was employed, it was purchased from Sekisui, Japan. The glass transition temperature T_g of non-plasticized PVB was about 348 K and the presence of plasticizer decreases T_g . The benzoyl peroxide was obtained from Sigma-Aldrich. The structure of PVB is shown in Fig. 1.

General procedure. About 35 g of poly(vinyl butyral) powder, and 2 g of benzoyl peroxide, were mixed. The internal mixer, from Brabender Company in Germany, was set at 75°C above the glass transition temperature of the material and mixed at 120 rpm for 20 min.

The used tablet should be prepared in the hot press device under the melting temperature of the material for 2 min. The arranged tablet was positioned in a rheometer

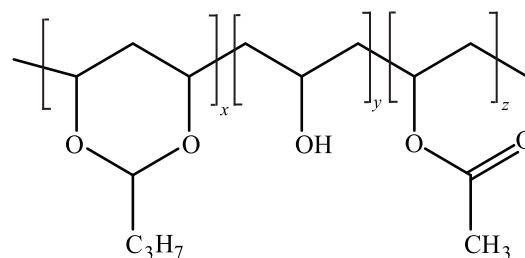


Fig. 1. Poly(vinyl butyral) monomers.

and then the two pans from top to bottom were aligned and rotated repeatedly at the same melting temperature (170°C). It provided two rows of data in terms of time comprising loss factor and capacity factor. By plotting the dissipation coefficient and capacity coefficient over time, the intersection point of these two graphs is the point of complete polymer curing time [15].

The frequency rheometer, MCR 302 model from Anton Paar Company in Swiss, has two bins, each with a separate temperature setting. Since the heat must pass through the bins then transfer to the molds and eventually reach the desired material, the set temperature should be adjusted to about 20% of the desired temperature, which is the melting temperature of the material. This device consists of two jaws that take the form of a clamp of the desired material and perform a tensile test by applying speed to the available software for the particular device. The software reports the stress-strain graph [16]. Finally, the chemical test including FTIR, SED, XRD, DCS and mechanical tests such as impact tests, tensile tests, Shore D hardness tests were performed.

RESULTS AND DISCUSSION

Investigating the internal mixing device diagram.

The variation of the mixing torque against time was displayed in Figs. 2a, 2b, which was attained for linear and cross-linked polymer treatment in the internal mixer. The results revealed that, in cross-linked polymer, the rising in mixing torque was higher and the time needed is lower considerably than linear ones. The mixing torque was increased by crosslinking the polymer. These results revealed that cross-linking has a substantial influence on the polymer structure. Increasing interfacial interaction and M_w originated from cross-linking can enhance the melt viscosity and consequently the mixing torque. The results showed that useful information can be attained through mixing torque–time curves.

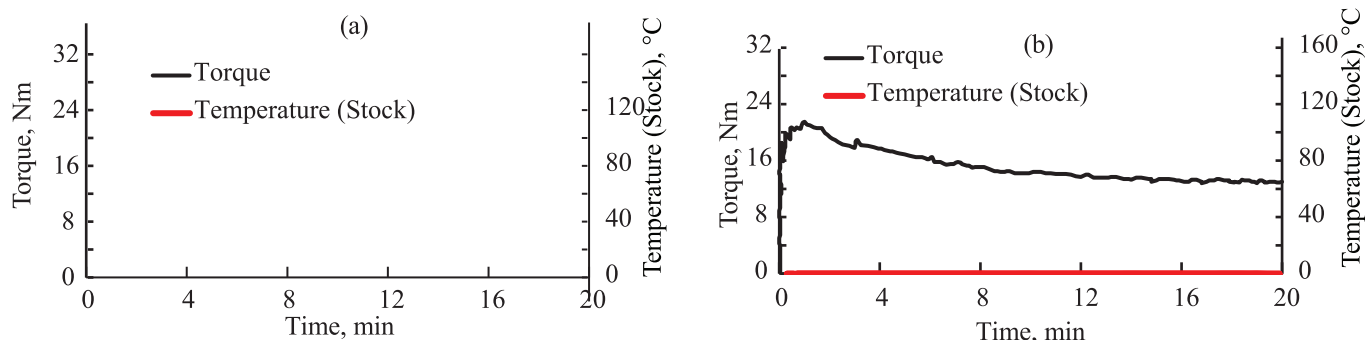


Fig. 2 (a) Torque-time linear polymer diagram. (b) Cross-linked polymer diagram.

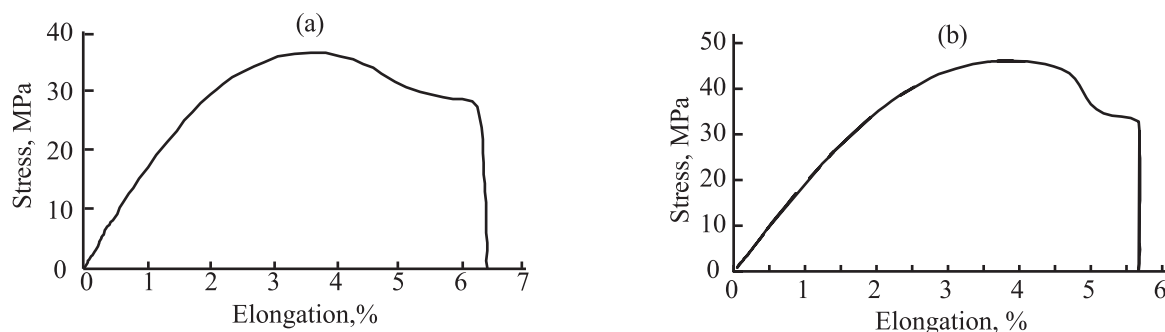


Fig. 3. (a) The stress-strain linear polymer, (b) the stress-strain cross-linked polymer.

As shown in Figs. 2a, 2b in the linear poly(vinyl butyral), there is less torque than the cross-linked polymer. Due to the viscosity formula in terms of torque and because the speed of both samples is the same, the cross-linked sample is more viscous.

$$U = C \frac{T - T_f}{9} \quad (1)$$

In the above equation (Eq. 1), the term U stands for viscosity, T denotes the torque in the diagrams of the device at the maximum point, also T_f denotes the torque which reaches a constant at the end of the applied time, v the velocity applied to the device in rpm, and C is the constant of the device.

Investigation of the tensile test. One of the most important characteristics of polymers is their inherent toughness and resistance to fracture (crack propagation). The mechanical properties of plastic materials depend on both the strain and temperature.

The results of the tensile test are expressed as a stress-strain graph. In Figs. 3a, 3b, the tensile test results were presented for linear and cross-linked polymer.

As expected, the elastomeric coefficient of polymer

increased by about 20% after the cross-linked process. The elastic modulus of the linear polymer is lower than that of the cross-linked polymer, which means that the cross-linked polymer exhibits greater resistance to deformation. The results also showed that the percentage of stretching of the cross-linked sample up to the yield point is slightly higher than that of the linear sample, while the cross-linked sample shows more traction at the breakpoint. Also, the cross-linked polymer showed more stress than the linear sample. Based on the toughness test, the model was able to absorb more energy until it was contested, these results are in agreement with the findings of Bai et al., in the study of poly(vinyl butyral)/graphene oxide composite [17].

The results of the hardness test. The hardness of a material is the resistance of a harder object to the formation of a trough. The most common method is the Shore hardness tester.

The Shore D Hardness test is named Durometer Hardness test and is used in the Rockwell tests. It is a standardized test containing measuring the depth of penetration of a precise indenter. The hardness test device is an STM-20 model from Santam Company in Iran according to the ASTM D2240 standard [18].

The amount of hardness was measured through the penetration of the Durometer indenter foot into the sample. Shore Hardness measures are without dimension and it goes between 0 and 100. The higher number signifies the harder substance. The resultant depth is reliant on viscoelasticity, hardness of the material, time of the test and shape of the indenter.

As presented in Table 1, the hardness test results were measured based on the polymer's resistance to crashes and it was repeated two times for accuracy.

As it can be seen, the two samples do not show much difference in resistance to indentation. Therefore, the impact test was used for further investigation.

The impact test results. The impact test is one of the standard approaches to determine the fracture energy of materials in dynamic stress. The foundation of the impact test is the determination of the amount of energy needed to break the component through impact [19]. The impact test device is STM-20 model from Yoshema Company in Japan.

The information obtained from this test is very useful in understanding how matter behaves in real applications. The purpose of the impact test is to simulate actual conditions to prevent failure and predict the failure of the sample. Two of the most important and common methods in impact testing are the Aizod and Charpy methods. The two methods differ only in the way the specimens are placed in the impact tester. The behavior of the substances vs. instantaneous load (impact) is very different from that of similar static load (tension).

It is clear from the results in Table 2 that the cross-linked polymer is more resistant to impact. These results are based on the ASTM-D256 standard, which is reported on three types of units [20].

The results of DSC tests. The DSC is a thermo-analytical technique in which the difference in the amount of heat required to raise the temperature of a sample and a reference is measured as a function of temperature. The DSC has two positions: one for sample placement and the other for placement of air, which is commonly used as a reference. Both locations are given a heat value to keep both at the same temperature.

The thermal properties were determined by DSC, performed at a heating rate of $20^{\circ}\text{C min}^{-1}$ in the temperature range of 0 to 280°C , and under a nitrogen atmosphere.

Table 1. Results of D-Shore hardness test

Sample	First sample	Second sample
Linear PVB	68	69
Cross-link PVB	69	70

Table 2. Results of impact tests

kJ/m ²	Units		Sample
	J/m	kg.f.cm	
1.08	12.11	0.4	Linear PVB1
1.12	13.03	0.47	Linear PVB2
2.17	22.76	0.76	Cross-linked PVB1
2.22	24.68	0.8	Cross-linked PVB2

The DSC is a method used to explore the reaction of polymers against heating (Fig. 4). It can investigate the melting of a crystalline polymer or the glass transition. The percentage of temperature variation for a certain quantity of heat will vary between the two pans. Amorphous polymers in the DCS diagram do not show crystallinity points or even melting points. Of course, there will be no melting point in the cross-linked polymers. Here, these graphs were used to investigate changes in the glass transition temperature.

As shown in the linear polymer diagram, the glass transition temperature is 63°C . But in the cross-linked diagram, the glass transition temperature is set at 70°C (middle diagram). Therefore the cross-linked polymer had a higher glass transition temperature than the linear polymer.

XRD study of polymers. The X-ray diffraction XRD, through CuK_{α} radiation ($\lambda = 0.15418 \text{ nm}$) with Rigaku Smart Lab3 model was employed and the specimens were examined in the angular range of 2θ , from 4° to 110° . X-ray spectroscopy for amorphous materials is not expected to see any crystallinity. It should be noted that amorphous polymers have been shown to retain their amorphous state after curing. In the cross-linked polymer, the small peaks can be seen, which is due to the production of small crystals from the baking operation. In the example in the 2θ at 46° , a small peak exists (Fig. 5).

The application of the XRD diagram of PVB nanocomposites was explored by other researchers.

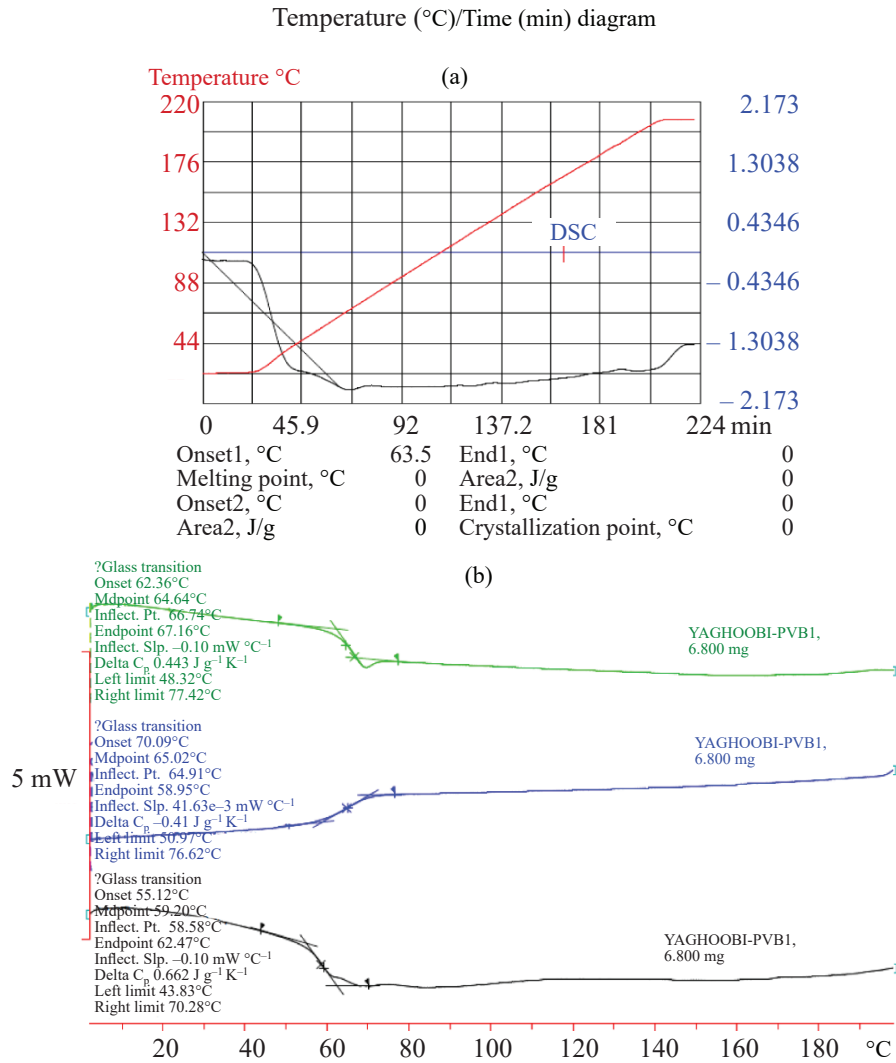


Fig. 4. (a) DSC diagram of linear polymer, (b) the DSC diagram of the cross-linked polymer.

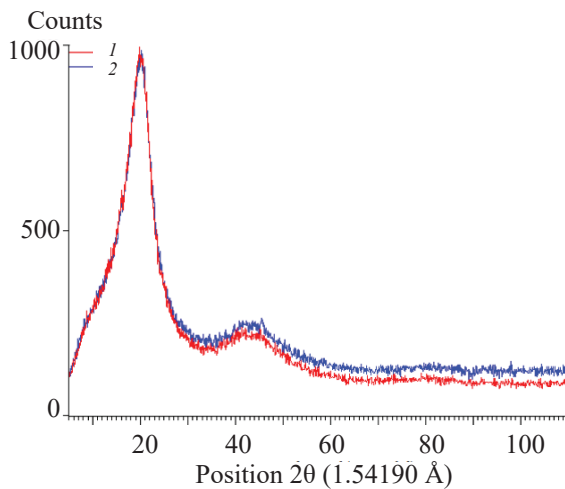


Fig. 5. XRD diagram of linear polymer (lower graph-red mark) and cross-linked polymer (upper graph-blue mark). (1) Yellow, (2) black.

Guinovart et al. had employed an XRD diagram to display the degree of exfoliation of the clay elements in the PVB structure. They realized that there is no crystalline peak in the XRD pattern of pure PVB, which discloses PVB as entirely amorphous; but by adding LiI to the PVB, the crystalline structure appeared in their XRD peaks. In addition, the amorphous and conductivity of the sample were decreased because the viscosity was increased and subsequently the movement of ions decreased [21].

Given that the used XRD in the present study may not have detected all the angles of diffraction, it can be said that the cross-linked polymer may have higher crystallinity in its texture.

Electron microscope results. The surface topographies of the samples were detected by SEM. In SEM analysis, a sample was scanned with an electron beam to create

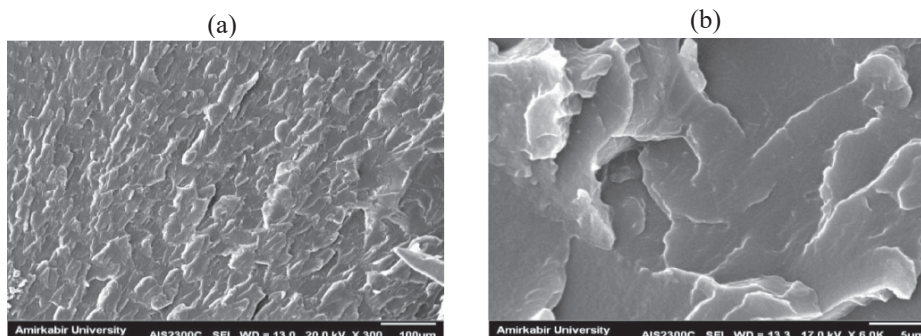


Fig. 6. SEM images of linear polymers.

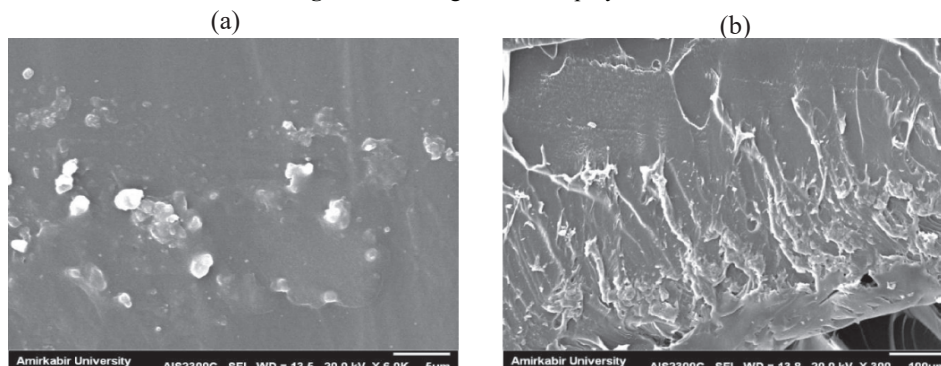


Fig. 7. SEM images of cross-linked polymers.

a magnified image for analysis. Different morphologies of the linear and cross-linked polymer are presented in Figs. 6a, 6b, 7a, 7b, respectively.

According to the SEM images of the cross-linked polymer, it was clear that their textures are more compact than the linear ones, in addition by comparing two SEM pictures of cross-linked and linear polymer, it was clear that in cross-linked ones the different parts of the surfaces are closer together.

Similar studies by other researchers confirmed that the addition of some polymeric compounds with each other or crosslinking them can increase the quality of the resulted polymer and SEM tests can help the researchers to judge this phenomenon. For example, Liu et al., have used SEM images to study the surface morphology of nanofibre with different PVB percent. Their results showed that different amounts of PVB can influence the morphology of the nanofibre [22]. Figures 6a, 6b, 7a, 7b show the SEM images of the linear and cross-linked poly(vinyl alcohol). The surface of the cross-linked polymer compared with the linear ones specifies a drop in the pore size. These findings were in agreement with the studies of Shafiei et al [23].

The cross-sectional picture of the cross-linked polymer displays that many bonds were formed between

the layers of poly(vinyl alcohol). Also, the SEM images displayed that the morphology of cross-linked polymer has an asymmetric structure that contains a compressed layer.

The infrared spectroscopy of the samples. The FT-IR spectroscopy 100 FTIR Model, from Perkin Elmer Spectrum, was employed to designate the functional groups of PVB in the range of 500–4000 cm^{-1} . The test was performed through KBr pellets and the output spectrums were logged in transmittance type vs. wavenumber. The molecular structure features of the samples were identified by FTIR spectra.

As investigated by Hajian et al., the synthesized PVB has different FT-IR peaks including; C–O–C stretching at 1138 cm^{-1} , CH_3 bending at 1377 cm^{-1} , CH_2 bending at 1435 cm^{-1} , aliphatic CH stretching peak at 2942 cm^{-1} , and OH- stretching vibration peak at 3390 cm^{-1} [24]. As suggested by Cho et al., the acetate peak is presented at 1736 cm^{-1} originated from the unreacted polyvinyl alcohol (PVA) subsequent from incomplete acetalization [25].

The functional groups present in the polymers can be identified due to the specific frequencies of the peaks.

Given that about 80–85% of the studied polymer is composed of vinyl butyral monomer, it is predicted that

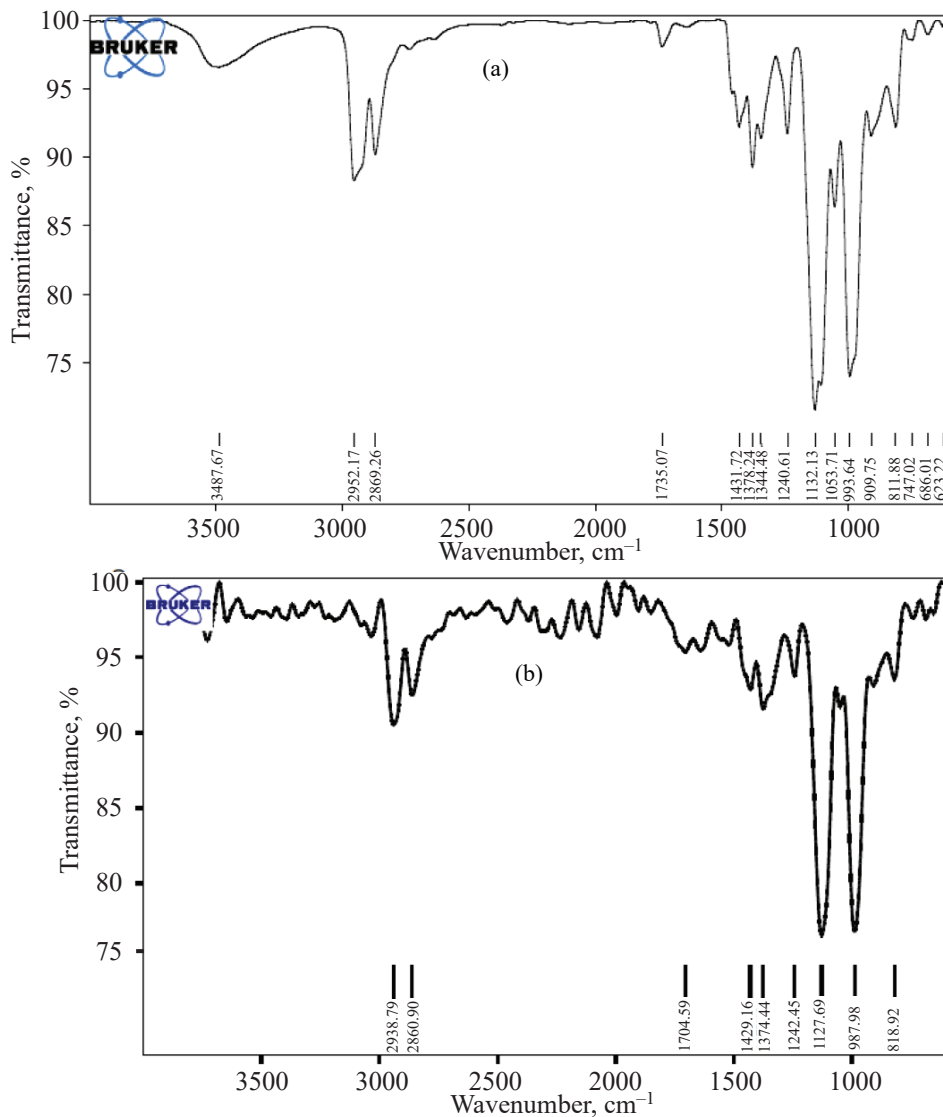


Fig. 8. (a) IR spectrum of linear polymer, (b) IR spectrum of cross-linked polymer.

there will be little difference in infrared spectroscopy and the signs were only at the points that the cross-linked links are formed. So, the diagram of the linear polymer was investigated at first and then it was compared with the result of the cross-linked polymer.

As can be seen, in the spectra obtained from cross-linked poly(vinyl butyral) (Fig. 8a) contrasting linear poly(vinyl butyral) (Fig. 8b), the OH bond is not seen at a wavenumber of about 3500 cm^{-1} because of annealing from this same functional group. On the other hand, because of the high annealing temperature, the possibility of forming a peroxide group due to low stability at this temperature and also bonding two oxygen atoms to the vinyl alcohol monomers is rejected. Finally, it can be

concluded that the bonding of the curing operation is affected through an ether bond or a single carbon-oxygen (C–O) bond because it has high stability. For introducing the more stable bond, a Hemi acetal carbon has been used to create a more stable bond. It is also noteworthy that the peaks appearing in the wavenumber of $2800\text{--}3000\text{ cm}^{-1}$ are related to the aliphatic carbon–hydrogen bond. The peak at $3000\text{--}3600\text{ cm}^{-1}$ signifies the hydroxyl group, that intensity has reduced in the cross-linked polymer.

The peaks appearing in the wavenumber between $1700\text{--}1750\text{ cm}^{-1}$ belong to the carbonyl group, which was not in the linear polymer (Fig. 8a). It was produced in the cross-linked polymer; similar interpretations were revealed by Hojjati et al. [26]. The peaks that appeared in

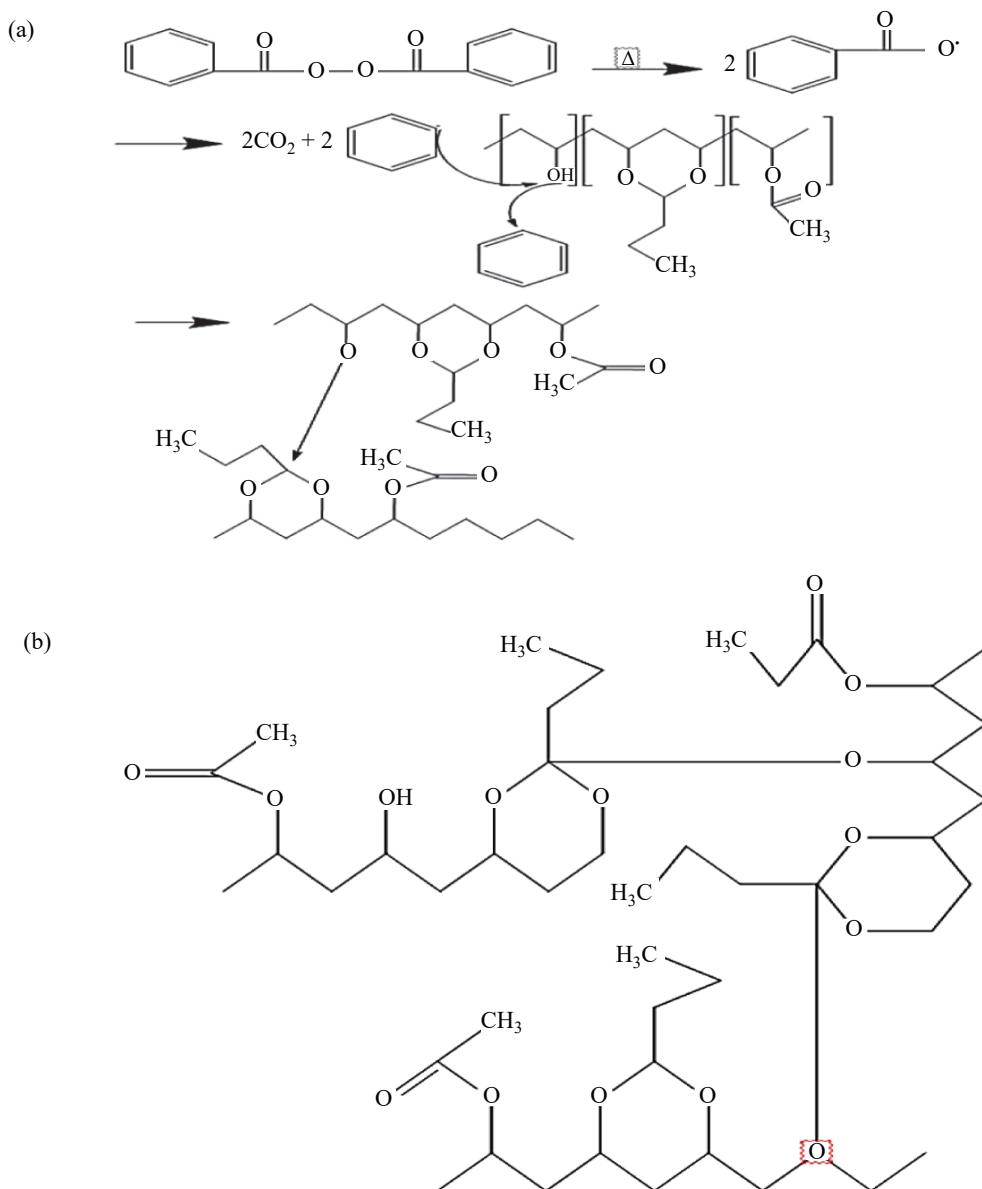


Fig. 9. Forming cross-link at first stage (a), and second stage (b).

wavenumber $1000\text{--}1550\text{ cm}^{-1}$ are to the ether bonds and the single carbon-oxygen bonds present in the polymer structure. It should be noted that all of these peaks exist in both diagrams and are identical. The only difference between the two diagrams relates to the absence of the hydroxyl group in the cross-linked polymer mentioned above. Similar studies were performed by Cordoba et al. [27]. Some researchers such as Aktürk and Zheng revealed that the peak at 1100 cm^{-1} is associated with the acetal groups (C–O–C), which intensity has improved in the studied polymer after cross linking [28, 29].

THE FINAL REACTION FOR CROSSLINKING

The crosslinking agents allow the functional monomers to bond with each other and remain firmly in place, after polymerization and molecular template separation. The type and size of crosslinking agent affect the morphology and mechanical stability of the cross-linked polymer.

The following reactions (Figs. 9a, 9b) were suggested through the interpretation of the FT-IR spectroscopy.

In the first step, the oxygen-oxygen bond of benzoyl peroxide is broken and converted to two radicals by



Fig. 10. Cross-linked polymer (right) and linear polymer (left).

heating. Because of the instability, this reaction continues and two carbon dioxide molecules are separated and the result is two benzyl radicals. Benzyl radicals will initiate baking by attacking the hydroxyl group on the vinyl alcohol monomer.

In the second step, after the separation of hydrogen from the hydroxyl group, the oxygen radical attacks the acetylated carbon in the vinyl butyral monomer and a cross-linked was formed.

The linear polymer consists of polymer chains; cross-linked polymer has either chains connected by links or a 3D structure. The properties are dramatically different. The linear polymer is soluble, exhibits a melting point, has a larger extension at break and typically is less thermally stable. On the other hand, cross-linked polymers are insoluble (depending on cross-linking density), do not exhibit melting, and are more thermally stable. In general, cross-linked polymers have better weather ability and stability, are more difficult to process and in general are not recyclable. The real pictures of linear and cross-linked polymer were presented in Fig. 10.

CONCLUSIONS

In this study, the crosslinking of PVB was happened due to more capability and advantages of cross-linked polymer than linear ones. The mechanisms for cross-linked formation in PVB structure were described. The properties of cross-linked polymer were investigated and compared with linear polymer.

The chemical test including FTIR, SEM, XRD, DCS and mechanical tests such as impact tests, tensile tests, and Shore D hardness tests were performed. According to the results, the cross-linked sample showed a greater elasticity up to the point of failure. In addition, the results

of the impact test showed that the cross-linked polymer could distribute better the force of impact. Through tensile test, it can be concluded that the cross-linked polymer endured more stress, exhibited greater toughness and was dense in color compared to the linear ones. In addition, after molding under a hot press machine, the cross-linked polymer clearly showed more adhesion than the linear polymer. The XRD diagram showed higher crystallinity in its texture than the linear one.

Also, for future works, using different amounts of benzoyl peroxide can be recommended for same polymer and other various peroxides. In the practical steps, the cross-linked sample clearly showed more adhesion so it could be used in adhesion to metals.

CONFLICT OF INTEREST

We declare that we have no conflict of interest.

REFERENCES

- Alva, G., Lin, Y., and Fang, G., *Mater. Chem. Phys.*, 2018, vol. 205, pp. 401–415. <https://doi.org/10.1016/j.matchemphys.2017.11.046>
- Cho, H., Rinaldi, R.G., and Boyce, M.C., *Soft Matter*, 2013, vol. 9, no. 27, pp. 6319–6330. <https://doi.org/10.1039/C3SM27125K>
- Elzière, P., Fourton, P., Demassieux, Q., Chennevière, A., Dalle-Ferrier, C., Creton, C., Ciccotti, M., and Barthel, E., *Macromolecules*, 2019, vol. 52, no. 20, pp. 7821–7830. <https://doi.org/10.1021/acs.macromol.9b01277>
- Ipackchi, H., Rezaoust, A.M., Esfandeh, M., and Rezaei, M., *Theor. Appl. Fract. Mech.*, 2020, vol. 105, p. 102406. <https://doi.org/10.1016/j.tafmec.2019.102406>
- Ambrosio, J.D., Sonogo, M., Staffa, L.H., Chinelatto, M.A., and Costa, L. C., *Compos. Part, B, Eng.*, 2019, vol. 175, p. 107118. <https://doi.org/10.1016/j.compositesb.2019.107118>
- Roy, A.S., Saravanan, S., Kishore, Ramamurthy, P.C., and Madras, G., *Polym. Compos.*, 2014, vol. 35, no. 8, pp. 1636–1643. <https://doi.org/10.1002/pc.22817>
- Gupta, S., Seethamraju, S., Ramamurthy, P.C., and Madras, G., *Ind. Eng. Chem. Res.*, 2013, vol. 52, no. 12, pp. 4383–4394. <https://doi.org/10.1021/ie3022412>
- Xu, Y., Luo, Y., Wang, F., Li, C., Wang, J., Zhu, H., and Guo, Y., *ChemistrySelect*, 2019, vol. 4, no. 29, pp. 8500–8507. <https://doi.org/10.1002/slct.201901498>

9. Feller, R.L., Curran, M., Colaluca, V., Bogaard, J., and Bailie, C., *Polym. Degrad. Stab.*, 2007, vol. 92, no. 5, pp. 920–931.
<https://doi.org/10.1016/j.polymdegradstab.2005.11.015>
10. Luckachan, G.E., and Mittal, V., *Cellulose*, 2015, vol. 22, no. 5, pp. 3275–3290.
<https://doi.org/10.1007/s10570-015-0711-2>
11. Jun, S., Choi, S. Bin, Han, C.J., Yu, Y.T., Lee, C.R., Ju, B.K., and Kim, J.W., *ACS Appl. Mater. Interfaces*, 2019, vol. 11, no. 4, pp. 4416–4424.
<https://doi.org/10.1021/acsami.8b20136>
12. Negishi, H., Yamaki, T., and Endo, A., *Microporous Mesoporous Mater.*, 2020, vol. 292, p. 109710.
<https://doi.org/10.1016/j.micromeso.2019.109710>
13. Bora, P.J., Azeem, I., Vinoy, K.J., Ramamurthy, P.C., and Madras, G., *Compos. Part B Eng.*, 2018, vol. 132, pp. 188–196.
<https://doi.org/10.1016/j.compositesb.2017.09.014>
14. Oo, H.Z., Kostromina, N., Osipchik, V., Kravchenko, T., and Yakovleva, K., *Int. J. Mater. Metall. Eng.*, 2019, vol. 13, no. 11, pp. 544–547.
15. Poudyal, H., Ahmed, I., and Chandy, A.J., *Int. Polym. Process.*, 2019, vol. 34, no. 2, pp. 219–230.
<https://doi.org/10.3139/217.3680>
16. Na, H., Zhao, Y., Zhao, C., Zhao, C., and Yuan, X., *Polym. Eng. Sci.*, 2008, vol. 48, no. 5, pp. 934–940.
<https://doi.org/10.1002/pen.21039>
17. Bai, Y., Zhang, J., Wen, D., Gong, P., and Chen, X., *Compos. Sci. Technol.*, 2019, vol. 170, pp. 101–108.
<https://doi.org/10.1016/j.compscitech.2018.11.039>
18. ASTM International. ASTM d2240-15: standard test method for rubber property-durometer hardness, 2015.
19. Thermoplastics Molding and Extrusion Materials, Standard Test Methods for Determining the Izod Pendulum Impact Resistance of Plastics, 2004.
20. ASTM D256 -10, Standard Test Methods for Determining the Izod Pendulum Impact Resistance of Plastics 10, 2018.
21. Guinovart, T., Crespo, G.A., Rius, F.X., and Andrade, F.J., *Anal. Chim. Acta*, 2014, vol. 821, pp. 72–80.
<https://doi.org/10.1016/j.aca.2014.02.028>
22. Liu, M., Turcheniuk, K., Fu, W., Yang, Y., Liu, M., and Yushin, G., *Nano Energy*, 2020, vol. 71, p. 104627.
<https://doi.org/10.1016/j.nanoen.2020.104627>
23. Shafiei, M., and Hajian, M., *Iran. Polym. J.*, 2019, vol. 28, no. 8, pp. 659–672.
<https://doi.org/10.1007/s13726-019-00732-4>
24. Hajian, M., Reisi, M.R., Koohmareh, G.A., and Jam, A.R.Z., *J. Polym. Res.*, 2012, vol. 19, no. 10, pp. 1–7.
<https://doi.org/10.1007/s10965-012-9966-6>
25. Rumyantsev, M., Rumyantsev, S., Kazantsev, O.A., Kamorina, S.I., Korablev, I.A., and Kalagaev, I.Y., *J. Polym. Res.*, 2020, vol. 27, no. 3, pp. 1–11.
<https://doi.org/10.1007/s10965-020-2031-y>
26. Hojjati, M.R., Bassanajili, S., and Forootan, A., *Iran. J. Chem. Chem. Eng.*, 2018, vol. 37, no. 1, pp. 175–183.
27. López-Córdoba, A., Castro, G.R., and Goyanes, S., *Mater. Sci. Eng. C*, 2016, vol. 69, pp. 726–732.
<https://doi.org/10.1016/j.msec.2016.07.058>
28. Aktürk, A., Erol Taygun, M., Karbancıoğlu Güler, F., Goller, G., and Küçükbayrak, S., *Colloids Surfaces A Physicochem. Eng. Asp.*, 2019, vol. 562, pp. 255–262.
<https://doi.org/10.1016/j.colsurfa.2018.11.034>
29. Zheng, Y., Yao, G., Cheng, Q., Yu, S., Liu, M., and Gao, C., *Desalination*, 2013, vol. 328, pp. 42–50.